Chitosan amphiphile coating of peptide nanofibres reduces liver uptake and delivers the peptide to the brain on intravenous administration

CrossMark

A. Lalatsa [a,1], A.G. Schätzlein [a,b], N.L. Garrett [c], J. Moger [c], Michael Briggs [d], Lisa Godfrey [a], Antonio Iannitelli [a], Jay Freeman [a], I.F. Uchegbu [a,b,*]

[a] UCL School of Pharmacy, 29-39 Brunswick Square, London WC1N 1AX, UK
[b] Nanomerics Ltd., 14 Approach Road, St. Albans, Hertfordshire AL1 1SR, UK
[c] School of Physics, University of Exeter, Stocker Road, Exeter EX4 4QL, UK
[d] GlaxoSmithKline, Pharmaceuticals R&D, Medicines Research Centre, Gunnels Wood Road, Stevenage SG1 2NY, UK

ARTICLE INFO

ABSTRACT

The clinical development of neuropeptides has been limited by a combination of the short plasma half-life of these drugs and their ultimate failure to permeate the blood brain barrier. Peptide nanofibres have been used to deliver peptides across the blood brain barrier and in this work we demonstrate that the polymer coating of peptide nanofibres further enhances peptide delivery to the brain *via* the intravenous route. Leucine[5]-enkephalin (LENK) nanofibres formed from the LENK ester prodrug – tyrosinyl[1]palmitate-leucine[5]-enkephalin (TPLENK) were coated with the polymer – N-palmitoyl-N-monomethyl-N,N-dimethyl-N,N,N-trimethyl-6-O-glycolchitosan (GCPQ) and injected intravenously. Peptide brain delivery was enhanced because the GCPQ coating on the peptide prodrug nanofibres, specifically enables the peptide prodrug to escape liver uptake, avoid enzymatic degradation to non-active sequences and thus enjoy a longer plasma half life. Plasma half-life is increased 520%, liver AUC_{0-4} decreased by 54% and brain AUC_{0-4} increased by 47% as a result of the GCPQ coating. The increased brain levels of the GCPQ coated peptide prodrug nanofibres result in the pharmacological activity of the parent drug (LENK) being significantly increased. LENK itself is inactive on intravenous injection.

1. Introduction

The difficulty in delivering molecules across the blood brain barrier (BBB) has been identified as the main reason for the limited development of neurotherapeutics [1]. Strategies to deliver peptides intravenously to the brain focus on: a) limiting peptide–hydrogen bonding with the blood water molecules and thus facilitating the partitioning of molecules into the lipid endothelial cell membranes of the BBB and b) stabilising the peptide against plasma degradation [2]. As such peptide brain delivery strategies revolve around structural modification methods to increase the peptide's lipophilicity, *e.g.* dimethylation of the tyrosine residue in D-pen[2]-D-pen[5]-enkephalin [3], chlorination of the phenyl alanine unit in D-pen[2]-D-pen[5]-enkephalin [4] or use of lipid prodrugs of D-ala[2]-D-leu[5] enkephalin (*e.g.* formation of the C-terminal cholesteryl ester and N-terminal amidation with 1,4-dihydrotrigonelline) [5]. However, increasing a drug's lipophilicity has been reported to result in increased plasma clearance and ultimately reduced brain exposure [6]

and so the use of lipidisation alone is not a sufficiently robust method of increasing brain exposure. Other peptide brain delivery methods include stabilising the peptide against degradation by cyclisation and preventing degradation by both carboxypeptidases and aminopeptidases, *e.g.* the cyclic peptide — D-Pen[2]-D-pen[5]-enkephalin [7]. However despite these published methodologies there are currently no marketed neuropeptide drugs and hence there is a need for a robust method of delivering peptides to the brain.

We have recently introduced a nanoparticle–peptide prodrug strategy in which the encapsulated lipidic peptide prodrug is stabilised against metabolic degradation and hence gives rise to a higher level of the actual peptide in the brain following both intravenous and oral administration [8]. The amphiphilic nature of the peptide prodrug is hypothesised to assist in its transcytosis across the BBB endothelial cells. We have also shown that a lipidised peptide prodrug — O-tyrosinyl[1]palmitate-D-Alanine[2]-leucine[5]-enkephalin (palmitoyl dalargin) forms nanofibres [9] and that these naked palmitoyl dalargin nanofibres deliver palmitoyl dalargin to the brain on intravenous injection, resulting in dalargin anti-nociceptive activity [10]. Dalargin alone, on intravenous injection, is not detected in the brain and is not active. As well as being used to deliver peptides to the brain [10], naked uncoated peptide nanofibres have been applied as tissue engineering scaffolds [11–14]. However, when used as drug delivery elements, and when peptide nanofibres are

---

* Corresponding author at: UCL School of Pharmacy, 29-39 Brunswick Square, London WC1N 1AX, UK. Tel.: +44 207 753 5998; fax: +44 207 753 5964.
E-mail address: ljeoma.uchegbu@ucl.ac.uk (I.F. Uchegbu).
[1] Present address: School of Pharmacy and Biomedical Sciences, University of Portsmouth, White Swan Road, Portsmouth, PO1 2DT, UK.

injected intravenously, 10–20% of the peptide nanofibre dose is found in the liver at the earliest time point [10]. Such liver deposition would reduce the drug available for brain uptake. We hypothesised that since N-palmitoyl-N-monomethyl-N,N-dimethyl-N,N,N-trimethyl-6-O-glycolchitosan (GCPQ) nanoparticles are not taken up by the liver [8], coating the nanofibre with GCPQ would divert the nanofibres from the liver resulting in a higher peptide blood residence time and increased brain uptake. We are aware that GCPQ nanoparticles also adhere to the luminal side of the blood capillaries [15] at the blood brain barrier and that such adherence would bring the nanofibres in close proximity to the target organ. We thus hypothesised that a GCPQ coating on peptide prodrug nanofibres would benefit brain drug delivery through a variety of mechanisms and set out to understand the function of the GCPQ coating on brain delivery. We have used the model leucine⁵-enkephalin (LENK) prodrug — tyrosinyl¹palmitate-leucine⁵-enkephalin (TPLENK), a peptide amphiphile that self assembles into nanofibres, to test our hypotheses.

2. Materials and methods

2.1. Materials

All reagents and chemicals were obtained from Sigma Aldrich Chemical Co., Poole, UK, unless otherwise stated. All solvents and acids were obtained from Fisher Scientific, Loughborough, UK. Dialysis membranes were purchased from Medicell International Ltd., London, UK. Deuterium oxide, Methanol-d4 and deuterated palmitic acid (palmitic acid-d31) were obtained from Cambridge Isotope Laboratories Inc., Cheshire, UK. Leucine⁵-enkephalin and tyrosinyl¹-palmitate-leucine⁵-enkephalin (TPLENK) were obtained from Peptisyntha Inc., Torrance, U.S.A. Water for injection was obtained from B. Braun Melsungen AG, Sheffield, UK. All reagents and chemicals were used without further purification and were ≥99% purity. Animals were purchased from Harlan, Oxfordshire, UK.

2.2. Synthesis and characterisation of chitosan amphiphiles — N-palmitoyl-N-monomethyl-N,N-dimethyl-N,N,N-trimethyl-6-O-glycolchitosan (GCPQ)

GCPQ amphiphiles of two different molecular weights 6–10 kDa and 50 kDa were synthesised and characterized as described previously by the acid degradation of glycol chitosan, the palmitoylation of acid degraded glycol chitosan with palmitic acid N-hydroxysuccinimide and finally alkylation of N-palmitoyl-6-O-glycolchitosan using methyl iodide [16]. GCPQ6, GCPQ10 and GCPQ50 were thus synthesised (Table 1). All polymers were characterized using proton nuclear magnetic resonance (¹H NMR) analysis and the NMR data used to estimate the level of palmitoyl grafting and N-methyl quaternary ammonium groups on the GCPQ polymers [17]. The molecular weights of the final polymers were determined using gel permeation chromatography and multiangle laser light scattering as previously described [16,18].

2.3. Nanofibre preparation and characterisation

For the hot plate, tail flick and pharmacokinetics mouse experiments, GCPQ–TPLENK formulations were prepared by probe sonicating (MSE Soniprep 150, MSE London, UK with the instrument set at 50% of

its maximum output) GCPQ and TPLENK in the presence of an aqueous solution of sodium chloride (0.9%w/v) [8], while TPLENK formulations were prepared by probe sonicating TPLENK in the presence of an aqueous solution of glycerol (2.25%w/v). For the Complete Freund's Adjuvant (CFA) rat experiments a higher dose of TPLENK was required and hence a more concentrated TPLENK formulation was prepared. Mice were dosed at 20 mg kg⁻¹, while rats were dosed at 30 mg kg⁻¹. Hence to prepare the rat formulations, GCPQ–TPLENK formulations were prepared by dissolving GCPQ and TPLENK in methanol (6 mL). The methanol was then removed by rotary evaporation to produce an amorphous thin layer of drug-polymer residue. Next, the solid preparation was left overnight under vacuum and reconstituted in water for injection BP and the homogenous suspension was then pH adjusted to pH 7 with NaOH (1 M). TPLENK alone formulations were prepared by bath sonicating for 30 min in a solution of glycerol (10% w/v). Formulations for the _in vivo_ studies were filtered (0.8 μm filter) prior to administration and analysed by high pressure liquid chromatography (HPLC) [8] for TPLENK content after filtration.

Formulations for _in vitro_ experiments were prepared in a similar manner to those used in the hot plate, tail flick and pharmacokinetics mouse experiments.

The zeta potential of the samples was determined (Malvern Nano-Zs, Malvern Instruments, Malvern, UK) by diluting the formulations (a 1 in 7 dilution) prior to conducting the measurement at room temperature. The viscosity of the formulation was assumed to be equivalent to the viscosity of water. Prior to measurements a zeta potential standard (Zeta transfer standard, DTS1230, Malvern, UK) was measured and the zeta potential was found to be in agreement with the value quoted by the manufacturer.

Particles were imaged by electron microscopy using methods previously reported [18].

Nanomedicine stability studies in plasma were conducted by incubating the formulations in plasma and analysing for TPLENK over time using methods previously reported.

For plasma protein binding studies, blood was collected from male CD-1 mice in sterile medical grade polyethylene terephthalate (PET) tubes, spray coated with tripotassium ethylenediamine tetraacetic acid (3.6 mg) and maintained on ice (4 °C) till the plasma could be separated by centrifugation (3350 g, 15 min at 4 °C, Hermle Z323 centrifuge, Hermle Labortechnik GmbH, Gosheim, Germany). Freshly prepared TPLENK formulations (4 mg mL⁻¹ of TPLENK and 10.4 mg mL⁻¹ of GCPQ, 20 μL) were incubated with plasma (180 μL) at 37 °C for 5 min [19]. A short incubation time was selected in order to avoid extensive peptide degradation in the plasma. TPLENK is stable over this period in plasma as we have shown previously [8]. Samples were centrifuged in polyallomer tubes (169,000 g, 45 min at 4 °C) using an Optima MAX-E Ultracentrifuge (Beckman Coulter UK Ltd., High Wycombe, UK). Immediately after centrifugation, the supernatant was diluted with methanol (600 μL) and analysed by HPLC using the isocratic method described previously [8]. The pellet was resuspended in methanol, dimethylsulfoxide (10:1 v/v, 220 μL) and was also analysed by HPLC [8].

2.4. In vivo studies

2.4.1. Animals

CD-1 male outbred mice (4–5 weeks old, weight = 20–26 g) were used for the pharmacokinetic and _ex-vivo_ imaging studies, Balb/C male

Table 1
TPLENK–GCPQ nanomedicines.

Samples	GCPQ Mn (kDa)	GCPQ polydispersity Index	GCPQ mol% palmitoyl groups	GCPQ mol% quaternary ammonium groups	Peptide–polymer nanofibres (1: 2.6 g g⁻¹) zeta potential (mV)	Appearance
TPLENK	N/A	N/A	N/A	N/A	−32.7 ± 0.06	Clear to slightly translucent
GCPQ6	5.62	1.091	20.0	12.4	18.8 ± 1.73	Very slightly translucent, yellowish
GCPQ10A	11.88	1.044	18.4	10.5	19.1 ± 1.04	Very slightly translucent, yellowish
GCPQ10B	9.11	1.410	15.1	15.1	19.8 ± 1.3	Slightly translucent
GCPQ50	41.65	1.473	10.6	11.1	16.8 ± 1.21	Translucent, mildly opaque

mice (4–5 weeks old, weight = 22–28 g) were used for the tail flick and hot plate pharmacodynamics studies and Sprague Dawley rats (6–8 weeks old, weight = 200–250 g) were used for the Complete Freund's Adjuvant (CFA) pharmacodynamics studies. The animals were housed in groups of 4 (rats) or 5 (mice) in plastic cages in controlled laboratory conditions with ambient temperature and humidity maintained at ~22 °C and 60% respectively and with a 12-hour light and dark cycle (lights on at 7:00 and off at 19:00). Food and water were available *ad libitum* and the animals were acclimatised for 5–7 days prior to experimentation and acclimatised to the procedure room for 1 h prior to testing (rats for the CFA model) or at least 20 h prior to testing (mice for the tail flick and hot plate models). All studies were conducted under a UK Home Office Licence and approved by the local ethics committee.

2.4.2. Pharmacokinetics

Groups of animals (n = 5) were intravenously administered with either sodium chloride (0.9% w/v, 200 μL), TPLENK nanofibres (4 mg mL^{-1}, 20 mg kg^{-1}) in glycerol (2.25%w/v) or GCPQ–TPLENK nanofibres in sodium chloride solution (0.9%w/v) composed of GCPQ (10.4 mg mL^{-1}) and TPLENK (4 mg mL^{-1}) and at a TPLENK dose of 20 mg kg^{-1}.

At various time points, mice were killed and the blood, brain and liver were sampled. The blood and liver are the main tissues to which GCPQ distributes on intravenous administration [8] and the brain is the target organ for these studies. Blood samples (0.5–0.9 mL per mouse) were collected into evacuated, sterile, spray coated with tripotassium ethylenediamine tetraacetic acid (3.6 mg), medical grade PET tubes. Plasma was separated from the blood by centrifugation (4800 rpm for 15 min at 4 °C, Hermle Z323 centrifuge, Hermle Labortechnik GmbH, Gosheim, Germany) and was stored at −80 °C until required for analysis. Brains (0.35–0.45 g) and livers (0.9–1.7 g) were recovered from mice and immediately frozen in liquid nitrogen (−80 °C) till required for analysis.

All tissues were homogenised by adding to each brain or liver HEPES buffer (0.1 M) (4 mL per gramme of tissue) and the tissues homogenised using a CryoPrep impactor (Covaris, Herts, UK). For some early time point brain samples, 14 mL of HEPES buffer was added per gramme of tissue. To an aliquot of the tissue homogenate (200 μL) was added an acetonitrile solution of the internal standard Donezepil (5 ng mL^{-1}, 400 μL). All the samples were orbitally agitated for 10 min and centrifuged at 3000 rpm for 10 min. A sample of the supernatant (100 μL) was transferred to a 96-well plate using TeMo (Tecan, Cernusco Sul Naviglio, Italy), the supernatant diluted with water (80 μL) and analysed by liquid chromatography–mass spectrometry (LC–MS) as described below. The extraction of TPLENK from brain and liver samples was performed immediately after homogenization to minimise the *in situ* degradation of TPLENK.

Plasma samples were diluted 1:2 using HEPES buffer (0.1 M) and a sample (190 μL) transferred into Micronic tubes using a Freedom Evo 75 (Tecan, Cernusco Sul Naviglio, Italy). Some early time point plasma samples were diluted with HEPES buffer using a 1:400 dilution (the 5 minute sample), a 1:100 dilution (the 10 minute sample) or a 1:50 dilution (the 25 minute sample) instead of a 1:2 dilution. To an aliquot of the diluted plasma (200 μL) was added an acetonitrile solution of the internal standard Donezepil (5 ng mL^{-1}, 400 μL). The samples were orbitally agitated for 10 min and centrifuged at 3000 rpm for 10 min. A sample of the supernatant (100 μL) was transferred to a 96-well plate using TeMo, the supernatant was diluted with water (80 μL) and analysed by liquid chromatography–mass spectrometry (LC–MS) as detailed below.

The plasma standard curve was prepared by a 1:2 dilution of blank plasma samples with HEPES buffer (0.1 M). An aliquot of the diluted plasma (190 μL) was transferred to Micronic tubes using a Freedom Evo 75. A stock solution (1 mg mL^{-1}) was prepared by diluting TPLENK with dimethylsulfoxide and this stock solution was used to prepare 11 standard solutions with concentrations in the range of 5–10,000 ng mL^{-1}. The standard solutions (10 μL) were used to spike volumes (190 μL) of the diluted blank plasma using a Freedom Evo 75. In this way a calibration curve for plasma was prepared within the range, 0.72 to 1430 ng mL^{-1}. For quality control purposes, two reference samples were produced by spiking a stock solution of TPLENK (1 μg mL^{-1}) in blank plasma or acetonitrile, water (1:1 v/v) in order to produce samples with a final concentration of 50 ng mL^{-1}. To each of these spiked TPLENK samples was added an acetonitrile solution of the internal standard Donezepil (5 ng mL^{-1}, 400 μL). The standards were then processed as described above, *i.e.* centrifuged, the supernatant isolated and diluted and analysed by LC–MS.

Blank brains and livers were weighed and to each brain or liver sample was added HEPES buffer (4 mL per gramme of tissue). The tissue samples were homogenised using the CryoPrep impactor (impact level 4). An aliquot of the homogenate (190 μL) was transferred to Micronic tubes and using a stock solution of TPLENK (1 mg mL^{-1}) standard solutions were prepared in acetonitrile, water (1:1 v/v) and aliquots of these standard solutions (10 μL) then used to spike the tissue homogenate samples (190 μL) using a Freedom Evo 75. In this way a standard curve was prepared within the range 1.25 to 2500 ng mL^{-1} for both liver and brain samples. To each of the spiked brain or liver samples was added an acetonitrile solution of the internal standard Donezepil (5 ng mL^{-1}, 400 μL). The samples were then processed as described above, *i.e.* centrifuged, the supernatant isolated and diluted and analysed by LC–MS.

LC–MS analysis was performed utilizing an Applied Biosystems (API4000) mass spectrometer in the positive-ion/Turbo Ionspray mode (Applied Biosystems, Streetsville, Canada). The source temperature was set at 600 °C. Samples (5 μL) were injected using Presearch PAL CTC Autosampler (CTC Analytics AG, Zwingen, Switzerland) and gradient elution followed using an Agilent HP 100 HPLC (Agilent Technologies, Waldbronn, Germany), which was connected to a Thermo Gold (Aqua) column (30 × 3 mm, particle size = 3 μm, Thermo Scientific, Runcorn, UK). The column temperature was set at 50 °C. The mobile phase flow rate was set at 1 mL min^{-1}. The mobile phase comprised: mobile phase A, consisting of formic acid: water (0.1:99.9 v/v) and mobile phase B consisting of formic acid: acetonitrile (0.1:99.9 v/v). The gradient elution sequence was: t = 0 min, 20% mobile phase B; t = 0.8 min, 90% mobile phase B; t = 1.8 min, 20% mobile phase B. The retention time for the analytes was: Donezepil = 0.85 min and TPLENK = 1.26 min. The identifying species were: Donezepil Q1/Q3 = 380.3/91.2 and TPLENK Q1/Q3 = 794.6/136.0.

The stability of TPLENK in biological matrixes and recovery were both tested prior to the start of the analyses and the recovery of TPLENK from spiked plasma, brain and liver samples was 94.5, 99.6 and 95.3% respectively.

The pharmacokinetic parameters of TPLENK nanofibres and GCPQ–TPLENK-nanomedicines were calculated by applying non-compartmental pharmacokinetic analysis to the plasma concentration-time data using MicroCal Origin 6.0 software (Microcal, Buckinghamshire, UK).

2.4.3. Multiphoton microscopy

Deuterated GCPQ10 (dGCPQ10, Mw = 11.97 kDa, Mn = 13.99 kDa) and deuterated GCPQ6 (dGCPQ6, Mw = 9.11 kDa, Mn = 8.57 kDa) were synthesised as previously described [16] and nanoparticles prepared as described above. Mice were intravenously injected with dGCPQ (10.4 mg mL^{-1}, 200 μL, 85 mg kg^{-1}) and were subsequently killed at various time points. Organs were harvested and stored in neutral buffered formalin (10% v/v, 15 mL). All samples for multiphoton imaging were placed between two glass coverslips using Parafilm spacers following the same procedure as described previously [16,20].

Coherent Anti-Stokes Raman Scattering (CARS) microscopy was performed using a custom built imaging system based on a modified commercial confocal laser scanning microscopy and a synchronised dual-wavelength picosecond laser source. Laser excitation was provided by

an optical parametric oscillator (OPO) (Levante Emerald, APE, Berlin) pumped with a frequency doubled Nd:Vandium picosecond oscillator (High-Q Laser Production GmbH). The pump laser generated a 6 ps, 76 MHz pulse train at 532 nm with adjustable output power up to 10 W. The OPO produced collinear signal and idler beams with perfect temporal overlap and provided continuous tuning over a range of wavelengths. The signal beam was used as the pump, ranging from 670 to 980 nm and the pump laser was used as the Stokes beam at 1064 nm. The maximum combined output power of the signal and idler was approximately 2 W and average power at the sample was between 15 mW and 30 mW. Two Photon Fluorescence (TPF) microscopy was undertaken using a mode-locked femtosecond Ti:sapphire oscillator (Mira 900D; Coherent, USA) which produced 100-fs pulses at 76 MHz. The central wavelength of the fs beam was 800 nm with an average power at the sample that was attenuated to between 5 and 30 mW.

Imaging was performed using a modified commercial microscope (IX71 and FV300, Olympus UK). To minimise light loss the galvanometer mirrors were replaced with silver mirrors and the tube lens was replaced with a MgF_2 coated lens. The laser beams were directed onto the scanning confocal dichroic which was replaced by a silver mirror with high reflectivity throughout the visible and near infrared regions (21010, Chroma Technologies, USA). All imaging was performed using a 60×, 1.2 NA water immersion objective (UPlanS Apo, Olympus UK).

The epi-CARS signal was collected using the objective lens and separated from the pump and Stokes beams by a long-wave pass dichroic mirror (z850rdc-xr, Chroma Technologies, USA) and directed onto a second R3896 photomultiplier tube at the rear microscope port. The CARS signal was isolated at the photodetector using a single bandpass filter centred at the anti-Stokes wavelength. The epi-detected TPF signal was detected in a similar manner, undergoing spectral separation from the 800 nm excitation beam by a dichroic mirror before being isolated by a band pass filter.

2.4.4. Pharmacodynamics

Two acute pain models (the tail flick bioassay and the hot plate method) and one chronic pain model [the Complete Freund's Adjuvant (CFA) model] were used. Antinociception in the tail flick bioassay and hot plate experiments was assessed in mice, following the intravenous injection of a sodium chloride control (0.9% w/v), TPLENK nanofibres in glycerol (2.25% w/v) or a GCPQ–TPLENK formulation in sodium chloride (0.9% w/v). Antinociception in the CFA experiments was assessed in rats following the administration of the vehicle (glycerol — 10% w/v) or a GCPQ–TPLENK formulation in pH adjusted (pH = 7) water for injection or TPLENK nanofibres in glycerol (10% w/v).

2.4.4.1. Tail flick bioassay. Antinociception was evaluated using the tail flick warm water bioassay [8,16] in which mice are subjected to a thermal stimulus over a 10 s time frame and their response latency (a sharp removal of the tail from the stimulus) to the thermal stimulus measured. Mice not responding within 5 s were excluded from further testing and the baseline latency was measured for all mice 2 h prior testing. The baseline latency was 2.44 ± 0.62 s. An analgesic responder was defined as one whose response tail flick latency was two or more times the value of the baseline latency and the times were expressed as a percentage of the maximum possible effect (MPE). A mouse showing a MPE was a mouse achieving the maximum tail flick latency to thermal stimuli of 10 s. Mice were evaluated by a female researcher.

2.4.4.2. Hot plate bioassay. The hot-plate bioassay was also used to assess antinociception after intravenous administration. A glass cylinder (16 cm high, 16 cm in diameter) was used to keep the mouse on the heated surface of a hot plate (Harvard Apparatus, Kent, UK) that was maintained at 60 ± 0.1 °C. The response latency times until the mouse first exhibited nociceptive behaviour (licking of the paw or an escape jump) were recorded using a digital stopwatch capable of measuring 1/100th of a second. The cut-off time was 30 s to avoid damage to

the animals' paws and animals were excluded from testing if they had baseline latencies greater than 15 s. Three repeated measurements were recorded for each time point, with 60 s between testing and the response times were then converted %MPE values in a similar manner as highlighted above. Mice were evaluated by a female researcher.

2.4.4.3. Complete Freund's adjuvant chronic pain model. Rats received an intraplantar injection of 100 μL of Complete Freund's adjuvant (CFA), (*Mycobacterium tuberculosis* heat killed suspended in 85% paraffin oil and 15% mannide monooleate 1 mg/mL) using a glass Hamilton syringe with a 25G needle. CFA caused hind paw oedema and mechanical hypersensitivity as evaluated 24 h after the CFA injection.

Mechanical hypersensitivity was evaluated as previously described [21]. Rats were individually placed on an elevated plastic mesh (0.5 cm² perforations) in a clear plastic cage. Two habituations to the evaluation chambers for at least 5 min duration each were performed on two different days. A baseline measurement was taken on test day pre-CFA. Mechanical hypersensitivity was assessed by the sensitivity to the application of von Frey hairs (Ugo Basile, Varese, Italy). The von Frey filaments (1.4, 2, 4, 6, 8, 10, 15, 26 g) were presented perpendicularly to the plantar surface of the injected paw in ascending order, and held in this position for 5 s with enough force to cause a slight bend in the filament. Positive responses included an abrupt withdrawal of the hind paw or response was noted if the paw was sharply withdrawn or there was flinching upon application of the hair. Once a positive withdrawal response was established, the paw was retested, starting with the next descending von Frey hair until no response occurred. The lowest amount of force required to elicit a response was recorded as the paw withdrawal threshold (g) [22].

Mechanical allodynia was defined as a significant decrease in withdrawal thresholds to von Frey filament application. The 26 g hair was selected as the upper limit cut-off for testing.

To test formulation effects on mechanical allodynia, rats were evaluated for thresholds 5 days after CFA injection; they were then randomised according to their threshold values and injected with formulations. Rats were evaluated by a female observer, blinded to the treatments.

2.5. Statistical analysis

Statistical analysis was performed *via* a one-way ANOVA test using Minitab 16 (Minitab Ltd., Coventry, UK) followed by Tukey's post-hoc test. A two-way ANOVA test was used to analyse the CFA data.

3. Results

3.1. Peptide nanofibre morphology

Aqueous dispersions of TPLENK and TPLENK–GCPQ, present as translucent nanoparticle dispersions containing peptide nanofibres (Table 1 and Fig. 1). Fibres are 0.5–2 μm in length and 20–30 nm in width. TPLENK nanofibres are anionic in nature at neutral pH (Table 1) and appear as twisted aggregates (Fig. 1c), while GCPQ– TPLENK formulations consist of positively charged nanofibres at neutral pH (Table 1) and were devoid of the periodic twists seen in the TPLENK alone formulations (Fig. 1). GCPQ–TPLENK nanofibres also presented as a less aggregated morphology (Fig. 1). Peptide amphiphiles have been shown to self assemble into nanofibres [9,10,23] and peptide nanofibres arise from the hydrophobic association of the peptide's hydrophobic units and the hydrogen bonding of the peptide amino acids in the peptide backbone to form a beta sheet, with the peptide beta sheet wrapping tightly around the peptide nanofibre shaft [10]. The inclusion of GCPQ coats the nanofibres, as evidenced by the shift in zeta potential from a negative to a positive value on inclusion of GCPQ (Table 1). These are the first reported images of polymer coated peptide nanofibres (Fig. 1a, b and d) and the first evidence of a polymer coating
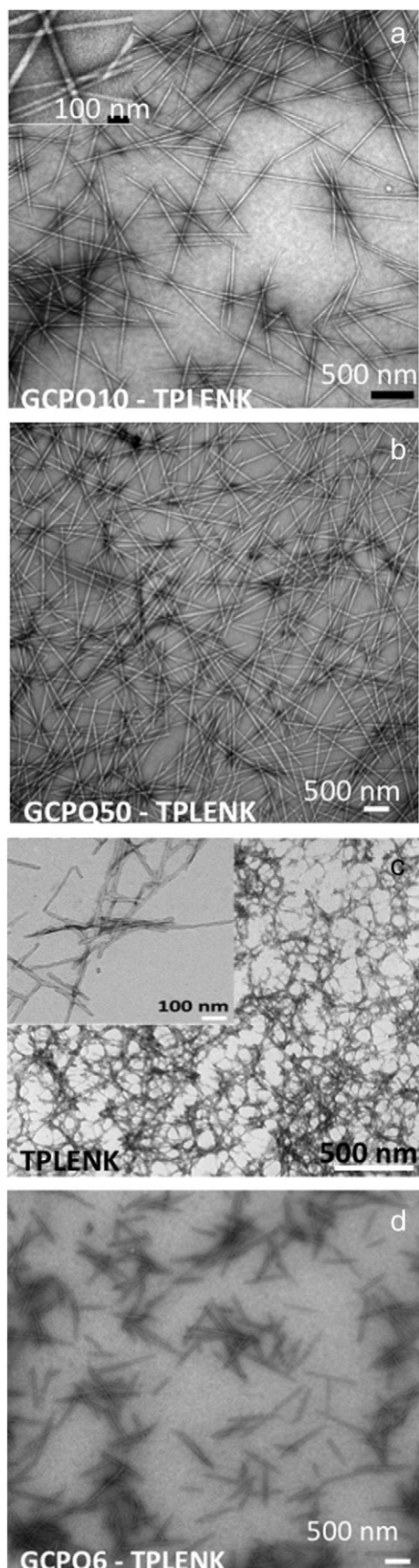
on nanofibres being achieved (Table 1). Specifically, Fig. 1 shows evidence that the nanofibre morphology persists even in the presence of a self assembling amphiphilic polymer, such as GCPQ. The GCPQ coating promotes spatial repulsion between individual fibres (Fig. 1), presumably *via* electrostatic repulsions (Table 1). The molecular weight (6–10 and 50 kDa) of the GCPQ coating does not affect the polymer coated nanofibre morphology.

3.2. Plasma stability of peptide nanofibres

LENK is a linear endogenous pentapeptide, which binds selectively to the delta opioid G-protein coupled receptors in the brain; the drug has a short plasma half-life of 3 min in humans after intravenous administration [24] and is degraded completely, in plasma *in vitro* studies, within 1.5 h [8]. Here we report that GCPQ50–TPLENK and TPLENK formulations do not undergo peptide degradation after an 8 h incubation period in plasma (Fig. 2a). This is in accordance with our previous report where we showed that TPLENK and GCPQ10–TPLENK formulations show exceptional *in vitro* stability in plasma [8]. It is clear, as we have established with palmitoyl dalargin nanofibres [10], that the nanofibre arrangement prevents access of peptidase enzymes to the peptide, preserving the peptide in the plasma.

Fig. 2b shows that the GCPQ coating also suppresses plasma protein binding as the amount of unbound peptide recovered in these *in vitro* experiments increases from 4% to over 16% in the presence of the polymer coating. A higher unbound fraction of the peptide nanofibres should improve across the blood brain barrier transport of the peptide prodrug.

3.3. Pharmacokinetics

Blood and tissues (brain and liver) were sampled at the following time points 5, 10, 25, 45, 90, 240, 480 and 1440 min but only the first 4 h are shown in Fig. 3, as tissue levels post the 240 minute time point were less than 0.05% of the peak values. We focused on the blood, brain and liver as the brain is the target organ and the intravenous injection of GCPQ nanoparticles results in distribution to the liver (2% of the injected dose) kidneys (6% of the injected dose) and bladder (4% of the injected dose) at the tmax (5 min) with less than 0.3% of the injected dose distributing to the other major organs (spleen, lungs, heart) [% dose = (tissue concentration X tissue weight) / dose weight] [8].

On intravenous injection, TPLENK nanofibres were cleared rapidly from the plasma with 6.4% of the dose found in the liver at the earliest time point and the TPLENK nanofibre formulation had a plasma half-life of 1.18 h (Table 2). This compares favourably with LENK's *in vivo* plasma half life of 3 min [24]. TPLENK also distributed to the brain with 0.07% of the injected dose present in the brain at the tmax (5 min). These levels compare well with the intravenous morphine which gives a peak level of 0.02% in the brain at the tmax (30 min) [25]. This brain delivery data is in line with data we have presented on palmitoyl dalargin nanofibres [10]. Palmitoyl dalargin nanofibres delivered palmitoyl dalargin to the brain on intravenous dosing and 0.2% of the intravenous dose is found in the brain at the tmax (5 min) [10]. It is thus clear that peptide nanofibres offer a robust method for delivering peptide drugs to the brain. What is not clear however is the exact mechanism of peptide nanofibre transcytosis across the brain endothelial cells and what proportion of the intact peptide nanofibres cross the

Fig. 1 Microscopy images of TPLENK formulations: a) transmission electron micrograph of GCPQ10 (10.4 mg mL^{-1})–TPLENK (4 mg mL^{-1}) nanofibres (GCPQ, TPLENK molar ratio = 0.017), b) transmission electron micrograph of GCPQ50 (10.4 mg mL^{-1})–TPLENK (4 mg mL^{-1}) nanofibres (GCPQ, TPLENK molar ratio = 0.005), c) transmission electron micrograph of TPLENK (4 mg mL^{-1}) nanofibres, d) transmission electron micrograph of GCPQ6 (10.4 mg mL^{-1})–TPLENK (4 mg mL^{-1}) nanofibres (GCPQ, TPLENK molar ratio = 0.36), All nanofibres are dispersed in NaCl solution (0.9% w/v) apart from TPLENK alone which is dispersed in glycerol solution (2.25% w/v).
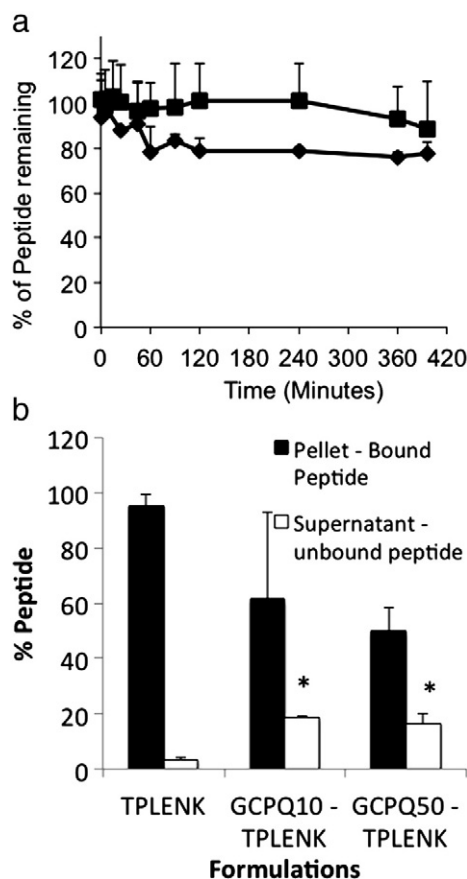
Fig. 2. *In vitro* peptide amphiphile stability (mean ± SD). a) The stability of GCPQ–TPLENK nanomedicines in plasma (50% v/v), ♦ = TPLENK (4 mg mL^{-1}), ■ = GCPQ50 (10.3 mg mL^{-1})–TPLENK (4 mg mL^{-1}). b) Plasma protein binding of GCPQ–TPLENK nanofibres [TPLENK (4 mg mL^{-1}) and GCPQ (10.4 mg mL^{-1})]. The peptide in the pellet is plasma protein bound while the peptide in the supernatant is the unbound fraction of the peptide. Significant differences * = p < 0.05 *versus* TPLENK.

brain endothelial cells and what proportion of disaggregated amphiphilic peptide monomers cross the brain endothelial cells.

Lipophilicity tends to increase the clearance of the drug from the plasma, once again limiting the amount of drug available for brain uptake [6]. The main plasma clearance organ is the liver and GCPQ (Mw = 10–20 kDa) is not taken up by the liver to an appreciable extent with about 2% of an intravenous dose of GCPQ nanoparticles present in the liver 5 min after dosing [8]. This level of liver uptake is low when compared to other intravenous injections of nanoparticle formulations. For example 40% of the doxorubicin sorbitan monostearate niosome dose is seen in the liver 10 min after intravenous dosing [26] and 55% of a liposomal albumin dose is found in the liver 10 min after intravenous dosing [27]. Based on the low level of liver uptake of GCPQ nanoparticles [8] we hypothesised that coating TPLENK nanofibres with GCPQ should prevent the liver uptake of TPLENK nanofibres. On coating TPLENK nanofibres with GCPQ10 and GCPQ50, plasma protein binding is reduced (Fig. 2b) and on administering TPLENK nanofibres coated with GCPQ10, liver AUC$_{0-4h}$ is reduced by 54%, plasma half-life is extended over 5 fold, and the brain AUC$_{0-4h}$ increased by 47% (Table 2, Fig. 3). With a GCPQ50 coating, the liver exposure of TPLENK was not significantly changed but the plasma half-life was extended over 300% and the brain AUC increased by 24% (Table 2, Fig. 3). Although animals were not perfused, the majority of the brain level measured was present in the brain parenchyma and not in the brain vasculature. This was confirmed by using published brain vasculature volumes of 12 μL per g^{-1} [28]. Using these values, the level of drug in the brain parenchyma at the earliest time point sampled, was estimated to be 66% of the overall brain level for TPLENK, 64% of the overall brain level for GCPQ10–

TPLENK and 62% of the overall brain level for GCPQ50–TPLENK. The increased distribution of TPLENK to the brain using GCPQ50–TPLENK and GCPQ10–TPLENK is due to the slower plasma clearance of these nanofibre formulations by various hepatic and extra-hepatic mechanisms. In the case of GCPQ10–TPLENK, there is an indication that the reduced hepatic clearance contributes to the higher level of TPLENK in the plasma from this formulation, as there is a significantly lower level of TPLENK in the liver when GCPQ10–TPLENK is administered when compared to the intravenous administration of TPLENK alone.

We have previously shown that GCPQ nanoparticles largely avoid the liver [8] and here we show for the first time that GCPQ10 coating of nanofibres also results in liver avoidance with only 1.6% of the intravenous dose of TPLENK being found in the liver at the earliest time point, on the intravenous injection of GCPQ10–TPLENK nanofibres (Fig. 3). This reduced uptake by the liver is one of the reasons for the improvement in brain permeation found for these nanofibers. GCPQ10–TPLENK nanofibres distribute more drug to the brain when compared to GCPQ50–TPLENK nanofibres (Fig. 3), with significant differences noted at the 10 minute time point, and one reason for this is the comparatively increased clearance of GCPQ50–TPLENK nanofibres by the liver (Fig. 3c).

3.4. CARS imaging

In order to understand the brain localisation of intravenously injected GCPQ nanoparticles we used CARS microscopy to image deuterated GCPQ nanoparticles. Using CARS microscopy [15,20], we visualised dGCPQ10 and dGCPQ6 particles in biological tissues after intravenous administration (Fig. 4). Fig. 4a and b shows the distribution of intravenously injected empty dGCPQ6 and dGCPQ10 nanoparticles distributed in the brain thalamus vasculature with some evidence of penetration into the brain parenchyma with dGCPQ10 nanoparticles (Fig. 4b). LENK is a mixed (δ and μ) opioid receptor agonist with a ten fold selectivity for the δ opioid receptor, when compared to the μ opioid receptor [29]. Mu opioid receptors are present in the thalamus and specifically the nucleus submedius of the medial thalamus and are partly responsible for the anti-nociceptive response [30]. Thus the appearance of dGCPQ10 and dGCPQ6 nanoparticles in the vasculature of the thalamus on intravenous administration should mean that intravenously injected GCPQ coated TPLENK nanoparticles should facilitate the delivery of TPLENK and in turn LENK to the site of these mu opioid receptors, with thalamus vasculature TPLENK crossing the brain endothelial cells and LENK being released by esterases. We have previously shown pharmacologically relevant mouse brain levels of LENK on intravenous administration of GCPQ10–TPLENK [8] and the localisation of the positively charged GCPQ10 nanoparticles to the luminal vascular walls of the mouse brain [31].

Delta opioid receptors are present in all regions of the central nervous system of humans with high levels in the cerebral cortex, nucleus accumbens and caudate nucleus [32]. Hence when considering translating this technology to humans, we have sufficient reason to assert that delta opioid receptors will also be accessible to intravenously injected TPLENK nanoparticles coated with GCPQ10.

Intravenously injected dGCPQ10 and dGCPQ6 nanoparticles are seen in the liver hepatocytes (Fig. 4c) and liver hepatocellular spaces (Fig. 4d) respectively. The appearance of dGCPQ10 nanoparticles within the liver hepatocytes demonstrates that the uptake of dGCPQ10 particles operates through different mechanisms when compared to most intravenously injected particles, which are found predominantly within the Kupffer cells [33] of the liver and are not normally detected in the hepatocytes. Kupffer cell localisation of other intravenously injected nanoparticles such as phospholipid liposomes is a result of opsonisation (labelling within the blood with blood proteins) and rapid clearance by the liver Kupffer cells [33,34]. The different uptake mechanism, experienced by GCPQ nanoparticles could be responsible for the very low liver
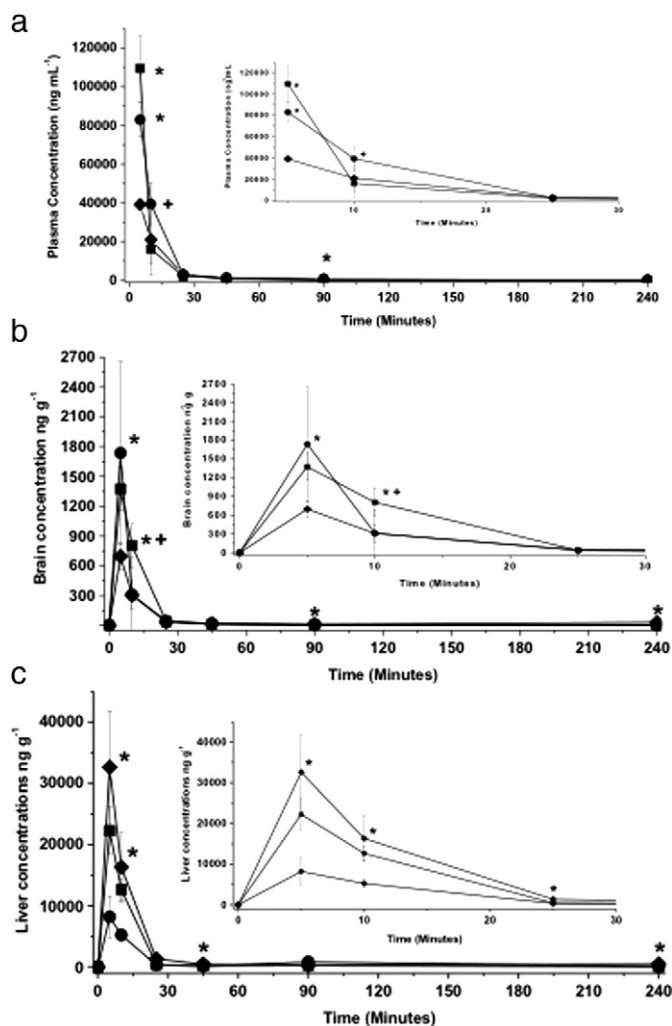
Fig. 3. The biodistribution of TPLENK nanofibre formulations after the intravenous administration of TPLENK nanofibres (20 mg kg^{-1}) to mice (mean ± s.d., n = 4): a) plasma levels following the administration of TPLENK (4 mg mL^{-1}) nanofibres (♦) in glycerol (2.25% w/w), GCPQ50 (10.4 mg mL^{-1})–TPLENK (4 mg mL^{-1}) nanofibres (■) in NaCl (0.9%w/v), GCPQ10 (10.4 mg mL^{-1})–TPLENK (4 mg mL^{-1}) nanofibres (●) in NaCl (0.9%w/v); b) brain levels following the intravenous administration of TPLENK nanofibres (20 mg kg^{-1}), symbols as in Fig. 3a; c) liver levels following the intravenous administration of TPLENK nanofibres (20 mg kg^{-1}), symbols as in Fig. 3a. * = Significant differences between TPLENK nanofibres and all GCPQ–TPLENK formulations (p < 0.05), + = Significant differences between GCPQ10–TPLENK and all other formulations (p < 0.05).

distribution of these nanoparticles [8]. These interesting results definitely warrant further study.

3.5. Pharmacodynamics

In an effort to understand whether the increased brain delivery of GCPQ–TPLENK formulations (Fig. 3b) would result in an increase in LENK activity, we evaluated the TPLENK formulations in both acute (tail flick and hot plate) and chronic (CFA) pain models (Fig. 5). All TPLENK formulations produced anti-nociceptive activity in the mouse tail flick bioassay and the GCPQ coated nanofibre formulations were more active than the TPLENK nanofibres alone (Fig. 5a). There was no anti-nociceptive activity recorded for the control samples (NaCl, GCPQ10 alone and LENK). While GCPQ50–TPLENK, GCPQ10–TPLENK and GCPQ6–TPLENK formulations all produced the maximum possible antinociception between 60 and 90 min after dosing (Fig. 5a), the activity of TPLENK nanofibres alone was inferior to that recorded for the GCPQ coated TPLENK nanofibre formulations.

GCPQ 10–TPLENK was also active in the hot plate assay (Fig. 5b). Once again LENK was not active in this assay. As can be seen from Fig. 5b, learning is observed during the hot-plate bioassay after 4 to 5 measurements [35] as evidenced by a change from a lick of the paws in test naive animals to an escape jump in less naive animals. This learning behaviour manifests as a progressive shortening of the jumping reaction time (Fig. 5c) and a disappearance of the licking behaviour.

GCPQ6–TPLENK was active in the CFA model whereas TPLENK alone was not active in this chronic pain model. GCPQ6 was used in the CFA assay instead of GCPQ10 or GCPQ50 as this polymer, being less viscous, enabled a higher concentration of TPLENK to be formulated (15 mg mL^{-1}) and thus a higher dose to be administered to the rat CFA model. The fact that TPLENK nanofibres show an inferior response when compared to the polymer coated nanofibre formulations provides further proof for the hypothesis that a polymer coating on peptide nanofibres promotes brain delivery of peptides.

Although with all TPLENK formulations, TPLENK was rapidly cleared from the plasma and the brain, with very low levels recorded 45 min after dosing (Fig. 3), anti-nociception after the administration of TPLENK formulations could be detected at the 25 minute time point and the activity peaked at the 60–90 minute time points (Fig. 5). This is explained by the fact that TPLENK is acting as a prodrug. We have previously shown that peak levels of LENK following the intravenous administration of GCPQ10–TPLENK were achieved at the 90 minute time point in accordance with the peak activity of the formulation [8]. The delayed pharmacodynamic response is further evidence that TPLENK is indeed acting as a prodrug. Ester prodrugs are rapidly cleaved to the parent drug: being completely cleaved within 30 min in the case of the phosphate ester prodrug of the anti-fungal agent, ravuconazole [36], or the (glycyl, glutamyl)diethyl ester prodrug of the anti-tumour agent, S-(N-p-chlorophenyl-N-hydroxycarbamoyl)glutathione [37].

4. Discussion

The delivery of peptides to the brain is an area fraught with difficulty due to the rapid degradation of peptides in the blood and brain and their hydrophilicity which prevents them crossing the BBB [1,38]. LENK is a case in point; LENK is a pentapeptide opioid receptor agonist with selectivity for the δ opioid receptors [29] and this drug is rapidly degraded and does not cross the blood brain barrier in sufficient quantities to be active; it is thus only active following intracerebroventricular administration at a high dose [39]. LENK is thus a good model to use to study peptide delivery. Our interest in this area has led us to introduce two new concepts: a) the use of nanofibre forming prodrugs [10] and b) a polymer encapsulated prodrug nanoparticle [8]. The prodrug nanofibre formulation of palmitoyl dalargin results in peptide prodrug nanofibres distributing to the brain and produces an anti-nociceptive response on intravenous administration, while dalargin is inactive via the intravenous route [10]. The LENK prodrug is TPLENK and this prodrug on encapsulation within chitosan amphiphile (GCPQ) nanoparticles, yields pharmacological levels of LENK on oral and intravenous administration, while LENK itself is inactive via the intravenous route [8]. In the current work we set out to examine the precise role of GCPQ in the GCPQ–TPLENK formulations. Here we hypothesised that the GCPQ in GCPQ–TPLENK formulations would result in an altered biodistribution of TPLENK, principally stemming from reduced liver uptake. This reduced liver uptake would eventually favour brain delivery of TPLENK and a pharmacological response. We have found that TPLENK forms nanofibres either alone or when coated with GCPQ (Fig. 1). Nanofibres are less aggregated when coated with GCPQ (Fig. 1a, 1b and 1d) and coated fibres are 1–2 μm in length and 20 nm in diameter. Nanofibres coated with GCPQ10 avoid liver uptake resulting in an increase in plasma residence and an increased delivery to the brain, increasing the plasma half life by over 5 fold and the brain exposure of TPLENK by 47% (Fig. 3 and Table 2). Coating the TPLENK nanofibres with GCPQ10 (molecular weight = 10 kDa) was preferable, with respect to brain delivery

Table 2
TPLENK intravenous dosing pharmacokinetics.

	Pharmacokinetic parameters	Intravenous administration of a 20 mg kg^{-1} dose		
		TPLENK	GCPQ10–TPLENK	GCPQ50–TPLENK
Plasma	AUC$_{0-4}$ (µg h mL^{-1})[a]	12.22	23.75	21.35
	Plasma C$_{max}$ (µg mL^{-1})	39.16	109.50	82.96
	t$_{1/2}$ (h)[b]	1.18	6.18	3.88
	Vd (L kg^{-1})[c]	2.72	7.40	5.07
	Clearance (L h^{-1} kg^{-1})	1.6	0.83	0.91
Brain	AUC$_{0-4}$ (µg h mL^{-1})	0.187	0.275	0.231
	Brain C$_{max}$ (µg g^{-1})	0.697	1.374	1.736
	Brain t$_{max}$ (h)	0.083	0.083	0.083
Liver	AUC$_{0-4}$ (µg h mL^{-1})	7.238	3.322	4.743
	Liver C$_{max}$ (µg g^{-1})	32.60	8.20	22.28
	Liver t$_{max}$ (h)	0.083	0.083	0.083

[a] AUC$_{0-4}$ — area under the concentration time curves 4 h post administration.
[b] t$_{1/2}$ — half-life.
[c] Vd — volume of distribution.

of TPLENK when compared to coating with GCPQ50 (molecular weight = 50 kDa) and the reason for this is unclear at present. Based on our current (Figs. 3 and 5) and previous [8] data, we know that TPLENK is rapidly converted LENK in the plasma and liver and that the prodrug TPLENK exerts its activity via the LENK parent drug.

Previous to our own work, peptides were converted to more hydrophobic variants to enable them to be delivered to the brain [3,4] and favourable results were not always guaranteed as lipidisation promotes drug clearance [6], depleting the plasma of drug and hence the brain of drug subsequently. The system that we have described involves forming a nanofibre with a cationic and amphiphilic liver avoiding polymer — GCPQ (which is eventually excreted by the kidneys) [8] to form the liver avoiding nanofibres with an extended plasma half life. The ultimate result is an increase in the level of coated peptide nanofibre in the blood and we know that this GCPQ coating promotes adhesion to the luminal vasculature surfaces of the brain [15], a fact that will bring these drug fibres in close proximity to the target site — the brain (Fig. 4b). This strategy produces increased brain delivery and activity from peptides, which are otherwise inactive on intravenous dosing.
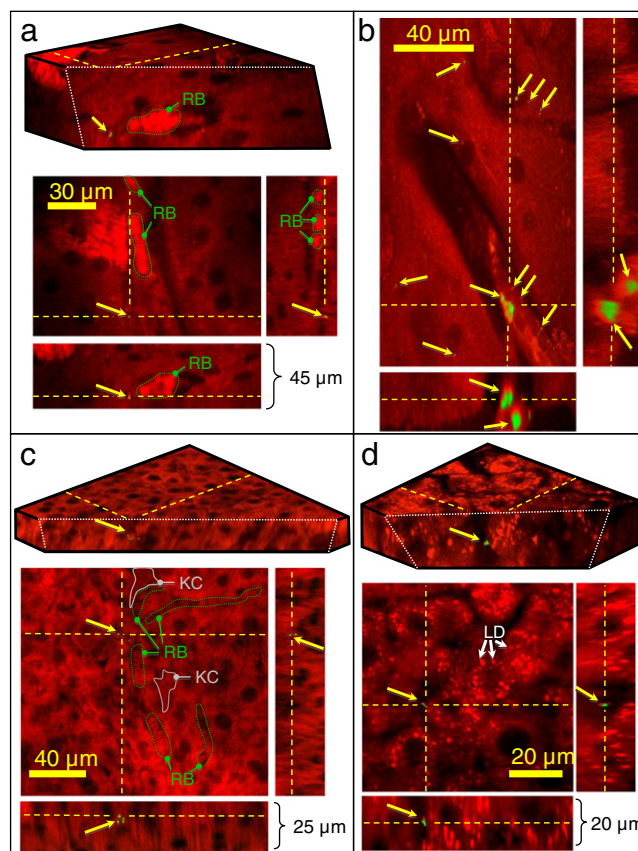
5. Conclusions

The use of lipidic ester peptide prodrug nanofibres coated with chitosan amphiphiles (GCPQ) is a viable strategy for the delivery of peptides to the brain following intravenous administration. These polymer coated nanofibres avoid plasma protein binding and liver uptake to deliver more of the peptide prodrug to the brain and produce a pharmacological response from peptides that are otherwise inactive via the intravenous route.
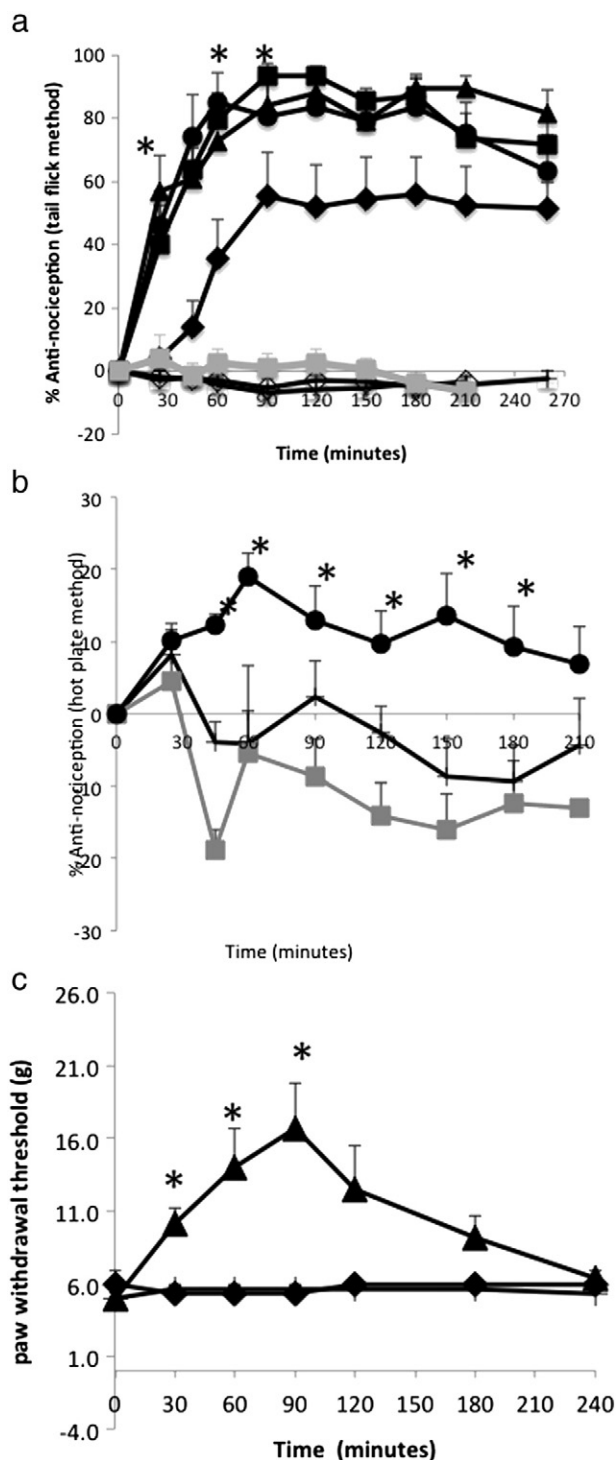
Acknowledgements

References

[1] A. Lalatsa, A.G. Schätzlein, I.F. Uchegbu, Drug delivery across the blood brain barrier, in: M. MurrayMoo-Young, M. Butler, C. Webb, A. Moreira, B. Grodzinski, Z. Cui (Eds.), Comprehensive Biotechnology, 2nd editionElsevier, Amsterdam, 2011, pp. 657–668.
[2] A. Lalatsa, A.G. Schatzlein, I.F. Uchegbu, Strategies to deliver peptide drugs to the brain, Mol. Pharm. 11 (2014) 1081–1093.
[3] D.W. Hansen, A. Stapelfeld, M.A. Savage, M. Reichman, D.L. Hammond, R.C. Haaseth, H.I. Mosberg, Systemic analgesic activity and delta-opioid selectivity in 2,6-dimethyl-Tyr1, D-Pen2, D-Pen5 enkephalin, J. Med. Chem. 35 (1992) 684–687.
[4] S.J. Weber, D.L. Greene, S.D. Sharma, H.I. Yamamura, T.H. Kramer, T.F. Burks, V.J. Hruby, L.B. Hersh, T.P. Davis, Distribution and analgesia of H-3 D-Pen2, D-Pen5 enkephalin and 2-halogated analogs after intravenous administration, J. Pharmacol. Exp. Ther. 259 (1991) 1109–1117.
[5] N. Bodor, L. Prokai, W.M. Wu, H. Farag, S. Jonalagadda, M. Kawamura, J. Simpkins, A strategy for delivering peptides into the central nervous system by sequential metabolism, Science 257 (1992) 1698–1700.
[6] E.V. Batrakova, S.V. Vinogradov, S.M. Robinson, M.L. Niehoff, W.A. Banks, A.V. Kabanov, Polypeptide point modifications with fatty acid and amphiphilic block copolymers for enhanced brain delivery, Bioconjug. Chem. 16 (2005) 793–802.

Fig. 4. Three-dimensional false-colour reconstructions of CARS (a, b and d) and TPF combined with CARS (c) microscopy images of mouse tissue samples after intravenous dosing with dGCPQ10L and dGCPQ6L nanoparticles [15,16]. Red contrast was obtained either from TPF or from CARS with the pump and Stokes beams tuned to excite the CH-stretch (2845 cm^{-1}), yielding strong signal from lipids within the sample and thus providing detailed sub-cellular structural information. Green contrast was obtained with the pump and Stokes beams tuned to excite the CD-stretch (2100 cm^{-1}), with strong signal detected from the dGCPQ. The weak signal from the non-resonant background in the green channel was several orders of magnitude less intense than the strong CD signal from the dGCPQ, and was therefore readily screened out by thresholding the images. By combining the red and thresholded green channels [15], it was possible to pinpoint co-localised signal arising from dGCPQ, thus allowing precise identification of the location of dGCPQ within the sample. a) Thalamus region of mouse brain, 60 min after an IV dose of dGCPQ6 (85 mg kg^{-1}, 10.4 mg mL^{-1}). Red blood cells (RBC) can be seen within a blood vessel (green arrows) as can the dGCPQ6 signal (yellow arrows) within the perivascular spaces. b) Thalamus region of mouse brain, 60 min after an IV dose of GCPQ10 (85 mg kg^{-1}, 10.4 mg mL^{-1}), with dGCPQ10 signal (yellow arrows) clearly seen in the brain parenchyma. c) Mouse liver 60 min after the intravenous dosing of GCPQ10 nanoparticles (85 mg kg^{-1}, 10.4 mg mL^{-1}), strong fluorescence signal from red blood cells resulting from increased autofluorescence as a result of fixation, is seen clustering within blood vessels (RB, green arrows) and the deuterated particle signal was found to be located within the cytoplasm of hepatocytes (yellow arrows). Kupffer cells (labelled KC) are outlined in grey to ease visualisation. d) Mouse liver 60 min after the intravenous dosing of dGCPQ6 nanoparticles (85 mg kg^{-1}, 10.4 mg mL^{-1}), lipid droplets are clearly seen (a selection of which have been labelled 'LDs' with white arrows) and the deuterated particle signal was found to be located within the hepatocellular spaces (yellow arrows). Since the deuterated signal contribution in dGCPQ arises only from the palmitoyl chain, there is still CH signal detected from the remaining CH$_2$ bonds within the nanoparticles, hence there is co-localised signal associated with dCGPQ in the red CH and the green CD images.

[12] C.E. Semino, J. Kasahara, Y. Hayashi, S. Zhang, Entrapment of migrating hippocampal neural cells in three-dimensional peptide nanofiber scaffold, Tissue Eng. 10 (2004) 643–655.

[13] R.G. Ellis-Behnke, Y.X. Liang, S.W. You, D.K. Tay, S. Zhang, K.F. So, G.E. Schneider, Nano neuro knitting: peptide nanofiber scaffold for brain repair and axon regeneration with functional return of vision, Proc. Natl. Acad. Sci. U. S. A. 103 (2006) 5054–5059.

[14] J. Guo, K.K. Leung, H. Su, Q. Yuan, L. Wang, T.H. Chu, W. Zhang, J.K. Pu, G.K. Ng, W.M. Wong, X. Dai, W. Wu, Self-assembling peptide nanofiber scaffold promotes the reconstruction of acutely injured brain, Nanomedicine 5 (2009) 345–351.

[15] N.L. Garrett, A. Lalatsa, D. Begley, L. Mihoreanu, I.F. Uchegbu, A.G. Schätzlein, J. Moger, Label-free imaging of polymeric nanomedicines using coherent anti-stokes raman scattering microscopy, J. Raman Spectrosc. 43 (2012) 681–688.

[16] A. Lalatsa, N. Garrett, J. Moger, A.G. Schatzlein, C. Davis, I.F. Uchegbu, Delivery of peptides to the blood and brain after oral uptake of quaternary ammonium palmitoyl glycol chitosan nanoparticles, Mol. Pharm. 9 (2012) 1764–1774.

[17] I.F. Uchegbu, L. Sadiq, M. Arastoo, A.I. Gray, W. Wang, R.D. Waigh, A.G. Schatzlein, Quaternary ammonium palmitoyl glycol chitosan — a new polysoap for drug delivery (vol 224, pg 185, 2001), Int. J. Pharm. 230 (2001) 77.

[18] A. Siew, H. Le, M. Thiovolet, P. Gellert, A. Schatzlein, I. Uchegbu, Enhanced oral absorption of hydrophobic and hydrophilic drugs using quaternary ammonium palmitoyl glycol chitosan nanoparticles, Mol. Pharm. 9 (2012) 14–28.

[19] S. Nakajima, T. Komuro, M. Shimamura, T. Hazato, Enkephalin-binding protein in human blood, Biochem. Int. 19 (1989) 529–536.

[20] N.L. Garrett, A. Lalatsa, I. Uchegbu, A. Schatzlein, J. Moger, Exploring uptake mechanisms of oral nanomedicines using multimodal nonlinear optical microscopy, J. Biophotonics 5 (2012) 458–468.

[21] S. Orita, T. Ishikawa, M. Miyagi, N. Ochiai, G. Inoue, Y. Eguchi, H. Kamoda, G. Arai, T. Toyone, Y. Aoki, T. Kubo, K. Takahashi, S. Ohtori, Pain-related sensory innervation in monoiodoacetate-induced osteoarthritis in rat knees that gradually develops neuronal injury in addition to inflammatory pain, BMC Musculoskelet. Disord. 12 (2011) 134.

[22] W.J. Dixon, Efficient analysis of experimental observations, Annu. Rev. Pharmacol. Toxicol. 20 (1980) 441–462.

[23] H. Cui, M.J. Webber, S.I. Stupp, Self-assembly of peptide amphiphiles: from molecules to nanostructures to biomaterials, Biopolymers 94 (2010) 1–18.

[24] M.A. Hussain, S.M. Rowe, A.B. Shenvi, B.J. Aungst, Inhibition of leucine enkephalin metabolism in rat blood, plasma and tissues in vitro by an aminoboronic acid derivative, Drug Metab. Dispos. 18 (1990) 288–291.

[25] W.A. Banks, A.J. Kastin, Opposite direction of transport across the blood–brain barrier for Tyr-MIF-1 and MIF-1: comparison with morphine, Peptides 15 (1994) 23–29.

[26] I.F. Uchegbu, J.A. Double, J.A. Turton, A.T. Florence, Distribution, metabolism and tumoricidal activity of doxorubicin administered in sorbitan monosterate (Span 60) niosomes in the mouse, Pharm. Res. 12 (1995) 1019–1024.

[27] G. Gregoriadis, B. Ryman, Fate of protein containing liposomes injected into rats, Eur. J. Biochem. 24 (1972) 484–491.

[28] I. van Rooy, S. Cakir-Tascioglu, W.E. Hennink, G. Storm, R.M. Schiffelers, E. Mastrobattista, In vivo methods to study uptake of nanoparticles into the brain, Pharm. Res. 28 (2011) 456–471.

[29] H.W. Kosterlitz, Enkephalins, endorphins and their receptors, in: C.A. Marsen, W.Z. Traczyk (Eds.), Neuropeptides and Neural transmission, Raven Press, New York, 1980.

[30] J.S. Tang, C.L. Qu, F.Q. Huo, The thalamic nucleus submedius and ventrolateral orbital cortex are involved in nociceptive modulation: a novel pain modulation pathway, Prog. Neurobiol. 89 (2009) 383–389.

[31] J. Moger, N.L. Garrett, D. Begley, L. Mihoreanu, A. Lalatsa, M. Lozano, M. Mazza, A. Schatzlein, I.F. Uchegbu, Imaging cortical vasculature with stimulated Raman

Fig. 5. The antinociceptive activity of TPLENK nanofibre, LENK and control formulations following intravenous administration (mean ± SEM, n = 10). A GCPQ, TPLENK weight ratio of 2.3 : 1 was used in all GCPQ–TPLENK formulations. For mouse (tail flick and hot plate) experiments the concentration and dose of LENK were 4 mg mL^{-1} and 14 mg kg^{-1} respectively while the concentration and dose of TPLENK were 4 mg mL^{-1} and 20 mg kg^{-1} respectively. For rat (CFA) experiments the concentration and dose of TPLENK were 15 mg mL^{-1} and 30 mg kg^{-1} respectively. For mouse experiments, all GCPQ and LENK formulations were administered in NaCl (0.9% w/v) and TPLENK alone was administered in glycerol (2.25% w/v). For rat experiments all GCPQ–TPLENK formulations were administered in pH adjusted water for injection, while TPLENK was administered in glycerol (10% w/v). a) The effect of GCPQ molecular weight on % antinociception observed with GCPQ–TPLENK formulations measured by the tail-flick bioassay: mice were dosed with NaCl (0.9% w/v, − + −), LENK (■), GCPQ10 (10.4 mg mL^{-1}, 85 mg kg^{-1} ◊); TPLENK nanofibres alone (♦); GCPQ6–TPLENK nanofibres (▲); GCPQ10–TPLENK nanofibres (●); GCPQ50–TPLENK nanofibres (■). * = Significant differences between GCPQ50–TPLENK, GCPQ10–TPLENK and GCPQ6–TPLENK formulations and all other formulations (p < 0.05), all TPLENK formulations were significantly different from the control formulations (NaCl, LENK and GCPQ10L alone, p < 0.05) b) % Antinociception measured by the hot plate method, symbols as in Fig. 5a. * = Significant differences between GCPQ10–TPLENK and all other formulations (p < 0.05), c) Paw withdrawal thresholds in a rat CFA model, rats had been administered CFA (0.1 mL via intraplantar injection) on Day 0 and mechanical hypersensitivity verified on Day 1, with an anti-nociceptive assessment (paw withdrawal threshold) carried out on Day 5, symbols as in Fig. 5a. * = Significant differences between GCPQ10–TPLENK and all other formulations (p < 0.05). TPLENK alone is inactive in this model.

[7] R.D. Egleton, T.J. Abbruscato, S.A. Thomas, T.P. Davis, Transport of opioid peptides into the central nervous system, J. Pharm. Sci. 87 (1998) 1433–1439.

[8] A. Lalatsa, V. Lee, J.P. Malkinson, M. Zloh, A.G. Schatzlein, I.F. Uchegbu, A prodrug nanoparticle approach for the oral delivery of a hydrophilic peptide, leucine(5)-enkephalin, to the brain, Mol. Pharm. 9 (2012) 1665–1680.

[9] A. Lalatsa, A.G. Schatzlein, M. Mazza, T.B. Le, I.F. Uchegbu, Amphiphilic poly(l-amino acids) — new materials for drug delivery, J. Control. Release 161 (2012) 523–536.

[10] M. Mazza, R. Notman, J. Anwar, A. Rodger, M. Hicks, G. Parkinson, D. McCarthy, T. Daviter, J. Moger, N. Garrett, T. Mead, M. Briggs, A.G. Schatzlein, I.F. Uchegbu, Nanofiber-based delivery of therapeutic peptides to the brain, ACS Nano 7 (2013) 1016–1026.

[11] G.K. Leung, Y.C. Wang, W. Wu, Peptide nanofiber scaffold for brain tissue reconstruction, Methods Enzymol. 508 (2012) 177–190.

scattering and two photon photothermal lensing microscopy, J. Raman Spectrosc. 43 (2012) 668–674.

[32] J. Peng, S. Sarkar, S.L. Chang, Opioid receptor expression in human brain and peripheral tissues using absolute quantitative real-time RT-PCR, Drug Alcohol Depend. 124 (2012) 223–228.

[33] D.C. Litzinger, A.M.J. Buiting, N. Vanrooijen, L. Huang, Effect of liposome size on the circulation time and intraorgan distribution of amphipathic poly(ethylene glycol)-containing liposomes, Biochim. Biophys. Acta Biomembr. 1190 (1994) 99–107.

[34] P.J. Photos, L. Bacakova, B. Discher, F.S. Bates, D.E. Discher, Polymer vesicles *in vivo*: correlations with PEG molecular weight, J. Control. Release 90 (2003) 323–334.

[35] D. Le Bars, M. Gozariu, S.W. Cadden, Animal models of nociception, Pharmacol. Rev. 53 (2001) 597–652.

[36] J.O. Knipe, K.W. Mosure, Nonclinical pharmacokinetics of BMS-292655, a water-soluble prodrug of the antifungal ravuconazole, Biopharm. Drug Dispos. 29 (2008) 270–279.

[37] E.M. Sharkey, H.B. O'Neill, M.J. Kavarana, H.B. Wang, D.J. Creighton, D.L. Sentz, J.L. Eiseman, Pharmacokinetics and antitumor properties in tumor-bearing mice of an enediol analogue inhibitor of glyoxalase I, Cancer Chemother. Pharmacol. 46 (2000) 156–166.

[38] A. Lalatsa, A.G. Schätzlein, I.F. Uchegbu, The blood brain barrier and drug transport, in: M.J. Alonso, N. Csaba (Eds.), Nanostructured Biomaterials for Overcoming Biological Barriers, Royal Society of Chemistry, London, 2012, pp. 329–482.

[39] J.D. Belluzzi, N. Grant, V. Garsky, D. Sarantakis, C.D. Wise, L. Stein, Analgesia induced *in vivo* by central administration of enkephalin in rat, Nature 260 (1976) 625–626.